HHS Public Access

Author manuscript

Acta Physiol (Oxf). Author manuscript; available in PMC 2022 May 01.

Published in final edited form as:

Acta Physiol (Oxf). 2021 May ; 232(1): e13640. doi:10.1111/apha.13640.

Zymogen-locked mutant prostasin (Prss8) leads to incomplete proteolytic activation of the epithelial sodium channel (ENaC) and severely compromises triamterene tolerance in mice

Daniel Essigke[1,*], **Alexandr V. Ilyaskin**[2,*], **Matthias Wörn**[1], **Bernhard N. Bohnert**[1,3,4], **Mengyun Xiao**[1], **Christoph Daniel**[5], **Kerstin Amann**[5], **Andreas L. Birkenfeld**[1,3,4], **Roman Szabo**[6], **Thomas H. Bugge**[6], **Christoph Korbmacher**[2], **Ferruh Artunc**[1,3,4]

[1]Department of Internal Medicine, Division of Endocrinology, Diabetology and Nephrology, University Hospital Tübingen, Germany

[2]Institute of Cellular and Molecular Physiology, Friedrich-Alexander University Erlangen-Nürnberg (FAU), Germany

[3]Institute of Diabetes Research and Metabolic Diseases (IDM) of the Helmholtz Center Munich at the University Tübingen, Germany

[4]German Center for Diabetes Research (DZD) at the University Tübingen, Germany

[5]Institute of Pathology, Department of Nephropathology, Friedrich-Alexander University Erlangen-Nürnberg (FAU), Germany

[6]Proteases and Tissue Remodeling Section, National Institute of Dental and Craniofacial Research, National Institutes of Health, Bethesda, Maryland, USA

Abstract

Aim: The serine protease prostasin (Prss8) is expressed in the distal tubule and stimulates proteolytic activation of the epithelial sodium channel (ENaC) in co-expression experiments *in vitro*. The aim of this study was to explore the role of prostasin in proteolytic ENaC activation in the kidney *in vivo*.

Methods: We used genetically modified knockin mice carrying a Prss8 mutation abolishing proteolytic activity (Prss8-S238A) or a mutation leading to a zymogen-locked state (Prss8-R44Q). Mice were challenged with low sodium diet and diuretics. Regulation of ENaC activity by Prss8-S238A and Prss8-R44Q was studied *in vitro* using the *Xenopus laevis* oocyte expression system.

Results: Co-expression of murine ENaC with Prss8-wt or Prss8-S238A in oocytes caused maximal proteolytic ENaC activation, whereas ENaC was activated only partially in oocytes co-expressing Prss8-R44Q. This was paralleled by a reduced proteolytic activity at the cell surface of Prss8-R44Q expressing oocytes. Sodium conservation under low sodium diet was preserved in

Address for correspondence: Ferruh Artunc, MD, University hospital Tübingen, Department of Internal Medicine, Division of Endocrinology, Diabetology and Nephrology, Otfried-Mueller-Str.10, 72076 Tübingen, Germany, ferruh.artunc@med.uni-tuebingen.de, Tel. +49-7071-2982711 / Fax +49-7071-2925215.

*shared first-authorship

Conflict of interests:
None.

Prss8-S238A and Prss8-R44Q mice but with higher plasma aldosterone concentrations in Prss8-R44Q mice. Treatment with the ENaC inhibitor triamterene over four days was tolerated in Prss8-wt and Prss8-S238A mice, whereas Prss8-R44Q mice developed salt wasting and severe weight loss associated with hyperkalemia and acidosis consistent with impaired ENaC function and renal failure.

Conclusion: Unlike proteolytically inactive Prss8-S238A, zymogen-locked Prss8-R44Q produces incomplete proteolytic ENaC activation *in vitro* and causes a severe renal phenotype in mice treated with the ENaC inhibitor triamterene. This indicates that Prss8 plays a role in proteolytic ENaC activation and renal function independent of its proteolytic activity.

Keywords

Prostasin; Prss8; epithelial sodium channel; ENaC; Prss8-S238A; Prss8-R44Q

Introduction

The epithelial sodium channel (ENaC) expressed in the distal nephron plays a decisive role in sodium homeostasis. Among many factors regulating ENaC-mediated sodium transport, channel activation through proteolytic processing by serine proteases is a specific feature of ENaC [1,2]. Proteolytic cleavage takes place at specific sites within the extracellular loops of the α- and γ-subunit (but not the β-subunit) and releases inhibitory tracts. This probably causes a conformational change of the channel favoring its open state [2,3]. During intracellular channel maturation cleavage occurs at two furin cleavage sites in α-ENaC and one in γ-ENaC. A final cleavage event probably takes place at the plasma membrane where γ-ENaC is cleaved by membrane-bound proteases and/or extracellular proteases in a region distal to the furin site. This latter cleavage event is thought to be essential for the conversion of near-silent channels into channels with a high open probability [4]. This concept is supported by the observation that proteolytic stimulation of ENaC-mediated whole-cell currents is associated with the appearance of a corresponding γ-ENaC cleavage product at the cell surface [4-7]. Moreover, recent evidence indicates that the most abundant γ-ENaC species in the apical membrane of rat and mouse kidney on a low salt diet is the twice-cleaved activated form [8]. The physiologically relevant proteases involved in proteolytic ENaC activation remain to be identified.

A potential candidate protease is prostasin (also known as Prss8 or CAP-1), because it has been demonstrated that co-expression of prostasin stimulates proteolytic ENaC activation in Madin-Darby Canine Kidney (MDCK) cells and *Xenopus laevis* oocytes [9-11]. Moreover, it has been reported that in humans urinary excretion of prostasin is increased in primary aldosteronism [12], in diabetic nephropathy with impaired renal Na^+ excretion [13] and in response to low Na^+ diet [14]. Prostasin is a glycosylphosphatidylinositol (GPI)-anchored membrane serine protease, which is highly expressed in the kidney tubule [15,16] in addition to prostate gland, colon, lung, salivary glands, pancreas, liver and skin [9,17]. The physiological role of prostasin in these tissues is largely unknown. Constitutive knockout of Prss8 leads to embryonic lethality probably due to placental insufficiency [18], and mice lacking Prss8 in the skin have an impaired epidermal barrier function and die within 60 h after birth due to dehydration [19].

The murine Prss8 gene encodes a protein consisting of 342 amino acid residues. During intracellular maturation the signal peptide consisting of the first 32 amino acid residues is removed from the N-terminus of the protein, which leads to the formation of a single-chain zymogen [20]. Formation of fully active prostasin requires zymogen cleavage after residue R44 resulting in a heavy and light chain linked by a disulfide bond. Mice with catalytically inactive prostasin due to replacement of serine by alanine in the catalytic histidine-aspartate-serine triad (Prss8-S238A [15]) or mice with a mutation of the activation site (zymogen-locked, Prss8-R44Q [16]) were found to be viable with largely preserved epidermal barrier function. Compared to the knock-out animals these mice had a rather mild phenotype with defects in whisker and pelage hair formation (Suppl. Fig 1). This demonstrates that essential *in vivo* functions of prostasin are independent of its proteolytic activity. This conclusion is supported by studies in *Xenopus laevis* oocytes which demonstrated that catalytically inactive mutants of prostasin were able to fully activate ENaC in co-expression experiments [21,22]. In contrast, mutating the catalytic triad of the channel activating protease 2 (CAP2 or Tmprss4) or matriptase (CAP3) abolished the stimulatory effect of these proteases on ENaC in co-expression experiments [21]. At present the conundrum that prostasin apparently does not require proteolytic activity to stimulate ENaC currents in the oocyte expression system remains an unresolved issue.

To investigate the *in vivo* relevance of prostasin for ENaC regulation in the kidney, we studied knockin mice carrying mutations of the prostasin gene that resulted either in proteolytically inactive (Prss8-S238A)[15] or zymogen-locked prostasin (Prss8-R44Q) [16]. In addition, we performed electrophysiological experiments with oocytes co-expressing murine ENaC with wild-type prostasin (Prss8-wt) or mutated prostasin (Prss8-S238A or Prss8-R44Q). We confirmed that co-expressing Prss8-wt or proteolytically-inactive prostasin Prss8-S238A with ENaC resulted in complete proteolytic channel activation. In contrast, zymogen-locked prostasin Prss8-R44Q only partially activated ENaC in co-expression experiments. Importantly, the reduced ability of Prss8-R44Q to cause proteolytic ENaC activation *in vitro* was reflected by an enhanced aldosterone secretion in response to dietary sodium restriction and by development of type 1 pseudohypoaldosteronism phenotype after pharmacological inhibition of ENaC *in vivo*.

Results

Coexpression of Prss8-wt or Prss8-S238 but not of Prss8-R44Q results in complete proteolytic activation of ENaC in Xenopus laevis oocytes

Using a cell surface biotinylation approach and Western blot analysis, we demonstrated that in the oocyte expression system Prss8-wt and Prss8-S238A are expressed at the cell surface in proteolytically-processed, i.e. mature form, whereas Prss8-R44Q remains in the uncleaved zymogen form as expected (Suppl. Fig. 2). In parallel experiments we investigated the effects of co-expressed Prss8-wt, Prss8-S238A or Prss8-R44Q on ENaC-mediated whole-cell currents. It is well known that in the oocyte expression system heterologously expressed ENaC reaches the cell surface not fully cleaved and can be further activated by extracellular application of prototypical serine proteases like trypsin or chymotrypsin [1,2]. Accordingly, we observed that application of chymotrypsin stimulated the amiloride-sensitive ENaC-

mediated whole-cell current by about 2-fold in oocytes expressing murine αβγENaC alone (Fig.1A and E). In oocytes co-expressing Prss8-wt (Fig. 1B) or Prss8-S238A (Fig. 1D) average baseline ENaC currents were significantly larger than those in oocytes expressing αβγ-ENaC alone (Fig. 1E). These increased ENaC currents could not be stimulated further by chymotrypsin (Fig. 1B, D-F), which indicates that the channels present at the cell surface are already fully cleaved. Co-expression of Prss8-R44Q also increased baseline ENaC currents (Fig. 1C and Fig. 1E), but this stimulatory effect appeared to be reduced compared to that of Prss8-wt or Prss8-S238A (Fig 1E). Importantly, in oocytes co-expressing ENaC and Prss8-R44Q application of chymotrypsin caused a further significant increase of ENaC currents by about 30% (Fig. 1C, E, F). Thus, in Prss8-R44Q co-expressing oocytes additional proteolytic channel activation by chymotrypsin is needed to stimulate ENaC currents to a similar level as in oocytes co-expressing Prss8-wt or Prss8-S238A. This clearly indicates that co-expression of Prss8-R44Q fails to fully cleave and activate ENaC unlike co-expression of Prss8-wt or Prss8-S238A.

Analysis of prostasin-specific proteolytic activity at the cell surface of oocytes co-expressing ENaC with Prss8-wt, Prss8-S238A or Prss8-R44Q

ENaC cleavage at the cell surface may be mediated by prostasin itself or by an endogenous protease activated by heterologous expression of prostasin. The latter hypothesis is supported by the finding confirmed above that the stimulatory effect of co-expressed proteolytically inactive Prss8-S238A on ENaC is similar to that of Prss8-wt [21]. Importantly, the stimulatory effects of Prss8-wt and of Prss8-S238A can be prevented by aprotinin [21,22], a known inhibitor of trypsin-like proteases. To distinguish between the specific proteolytic activity of prostasin and that of endogenous proteases at the cell surface, we used two different fluorogenic substrates: Ac-KHYR-AMC with an optimal substrate sequence for prostasin [23] and Boc-QAR-AMC which is suitable to detect proteolytic activity of a broad range of trypsin-like proteases [24,25]. Results from a typical experiment with Ac-KHYR-AMC are shown in Fig. 2A. A small decline of the fluorescence signal over time was observed in control oocytes expressing ENaC alone and in oocytes co-expressing ENaC with Prss8-S238A or Prss8-R44Q. This decay was also observed in control experiments without oocytes (data not shown) and therefore can be attributed to photobleaching of the fluorophore. In contrast, the fluorescence signal increased over time when Ac-KHYR-AMC was added to oocytes co-expressing ENaC with Prss8-wt (Fig. 2A). This indicates that heterologous expression of Prss8 results in detectable prostasin-specific proteolytic activity at the cell surface, which is absent in ENaC expressing control oocytes or in oocytes co-expressing ENaC with Prss8-S238A or Prss8-R44Q. In some experiments the fluorescence increase due to Prss8-wt expression was concealed by the concomitant fluorescence decline due to photobleaching. However, in all experiments the fluorescence signal detected after an incubation period of three hours was significantly higher in oocytes co-expressing ENaC and Prss8-wt than in oocytes expressing ENaC alone or co-expressing ENaC with Prss8-S238A or Prss8-R44Q. To compensate for the fluorescence decline due to photobleaching and to summarize data from similar experiments, fluorescence values were normalized at each time point to the average fluorescence signal detected in the corresponding control oocytes expressing ENaC alone (Fig. 2B). In summary these data indicate that prostasin-specific cell

surface proteolytic activity is detectable in oocytes co-expressing ENaC and Prss8-wt, but not in oocytes co-expressing ENaC with Prss8-S238A or Prss8-R44Q.

Stimulation of an endogenous trypsin-like protease activity is impaired in oocytes co-expressing ENaC with Prss8-R44Q

We hypothesized that heterologous expression of Prss8-wt, Prss8-S238A or Prss8-R44Q stimulates endogenous protease activity at the cell surface, possibly to different degrees. In the representative experiment shown in Fig. 2C a strong increase of the fluorescence signal due to Boc-QAR-AMC cleavage was observed in oocytes co-expressing ENaC with Prss8-wt or with Prss8-S238A. This is consistent with our functional data that in these two groups of oocytes proteolytic ENaC activation was complete without a further stimulatory effect of chymotrypsin. In contrast, in oocytes expressing ENaC alone the fluorescence signal did not increase but slowly declined over time probably due to photobleaching. Thus, in ENaC expressing control oocytes no trypsin-like proteolytic activity was detectable with Boc-QAR-AMC which is consistent with our functional data that the channel is not fully active in these oocytes and can be further stimulated by application of chymotrypsin.

Importantly, at the cell surface of oocytes co-expressing ENaC and Prss8-R44Q only a minor trypsin-like proteolytic activity was detectable with Boc-QAR-AMC as illustrated by the representative experiment shown in Fig. 2C. Normalized summary data from similar experiments demonstrate that on average the fluorescence signal obtained with Boc-QAR-AMC was significantly higher in oocytes co-expressing ENaC with Prss8-R44Q than in control oocytes expressing ENaC alone (Fig. 2D). However, the fluorescence signal resulting from Prss8-R44Q expression was much smaller than that observed in oocytes co-expressing ENaC with Prss8-wt or Prss8-S238A. This reduced activity in oocytes co-expressing Prss8-R44Q is in good agreement with our functional data that co-expression of Prss8-R44Q causes incomplete proteolytic ENaC activation with modestly increased baseline currents and a partially preserved stimulatory effect of chymotrypsin.

Prss8 is expressed in the proteolytically processed form in kidneys from Prss8-wt and Prss8-S238A mice

To investigate the *in vivo* relevance of the results obtained in the oocyte expression system, we used mice with the corresponding point mutations of the *prss8* gene which were described earlier [15,16]. Using Western blot analysis protein expression of prostasin was assessed in renal tissue from Prss8-wt, Prss8-S238A and Prss8-R44Q mice maintained on standard diet. In native protein samples relatively broad bands were detected at ~39 kDa in Prss8-wt and Prss8-S238A mice and at ~41 kDa in Prss8-R44Q mice (Fig. 3A, left). These results were reminiscent of the results in the oocyte expression system (Suppl. Fig. 2), indicating that the two bands correspond to the zymogen and to the heavy chain of proteolytically processed prostasin after dissociation of the disulfide bond under reducing conditions. When samples were pre-treated to remove N-glycosylation, the detected bands became narrower and migrated at ~26 kDa in Prss8-wt and Prss8-S238A mice and at ~28 kDa in Prs8-R44Q mice. Recombinant $Prss8^{30-289}$ as control migrated at ~37 kDa without and at ~25 kDa after deglycosylation. The densities of the prostasin band in Prss8-S238A mice were similar to that in Prss8-wt mice but were slightly increased in Prss8-R44Q mice

(Fig. 3B, C). Matriptase, also known as suppressor of tumorigenicity 14 protein (ST14), is an autoactivating type II transmembrane serine protease that has been reported to be a candidate for prostasin activation [16,26]. Its expression at the protein level was similar in all genotypes indicating that there was no compensatory up-regulation of matriptase in Prss8-R44Q mice (Suppl. Fig 3). Overall, these results show that prostasin is proteolytically processed in Prss8-wt and Prss8-S238A but not in Prss8-R44Q mice under control conditions in kidney tissue *in vivo*.

In addition, urinary prostasin excretion, which is supposed to serve as a surrogate for renal prostasin expression after shedding into the urine [12,27], was measured using an ELISA. As shown in Figure 3D, there was no difference of the creatinine-normalized urinary prostasin excretion between the genotypes under control conditions.

Sodium preservation requires hyperaldosteronism in Prss8-R44Q mice

To investigate the impact of prostasin on ENaC-mediated sodium handling *in vivo*, we studied Prss8 mutant mice under control conditions and when animals were challenged with a low sodium diet. Compared to Prss8-wt mice, Prss8-S238A and Prss8-R44Q mice had slightly increased sodium and potassium excretion under a control diet (Fig. 4A/B), which could be explained by increased food intake (Suppl. Fig. 4A). This is most likely a consequence of higher energy expenditure for thermoregulation in the presence of hair defects (Suppl. Fig. 1). Fluid intake, urine output and urinary creatinine excretion were not different in Prss8-R44Q mice and Prss8-S238A mice compared to Prss8-WT (Suppl. Fig. 4B-D). A low sodium diet with normal potassium (LS/NK) was followed by adequate lowering of urinary and fecal sodium excretion as well as mild increase in kaliuresis (Fig. 4A/B, Suppl. Fig. 4E). Loss of body weight was less than 5% in Prss8-S238A and Prss8-R44Q mice and similar to what was observed in controls (Fig. 4C). To further challenge ENaC-mediated sodium transport we combined the low sodium diet with high potassium intake (LS/HK). This diet has been shown to induce salt wasting and hyperkalemia in mice lacking mammalian target of rapamycin 2 (mTORC2) in the distal nephron [28]. As shown in Fig. 4B/C, the LS/HK diet increased K^+ excretion in all genotypes but did not induce salt wasting with body weight loss in Prss8-S238A and Prss8-R44Q mice. Plasma sodium, potassium and urea concentrations were not appreciably altered in Prss8-wt and Prss8-S238A mice under all diets (Suppl. Fig 4F-H). In Prss8-R44Q mice, plasma potassium concentration under control diet was slightly lower and significantly increased during a low sodium and particularly low sodium/high potassium diet without reaching hyperkalemia >5 mM (Suppl. Fig. 4G). Notably, low sodium and particularly low sodium/high potassium diet was followed by increased urinary creatinine excretion in all genotypes suggesting glomerular hyperfiltration (Suppl. Fig. 4D).

The course of the plasma concentrations of aldosterone after switch to a LS/NK and LS/HK diet is shown in Fig. 4D. Under control diet aldosterone levels were not significantly different in the three genotypes, but there was a trend towards slightly elevated aldosterone levels in Prss8-R44Q mice. In all genotypes plasma aldosterone concentrations were increased after two days of low sodium diet (LS/NK), but within five days declined back towards normal values in Prss8-wt and Prss8-S238A mice whereas significant

hyperaldosteronism persisted in Prss8-R44Q mice (Fig. 4D). In the latter, there was a tendency towards higher aldosterone secretion under a LS/HK diet that similarly persisted until day 5.

Prss8-R44Q but not Prss8-S238A mice are intolerant to continuous ENaC inhibition

We investigated ENaC-mediated sodium transport in Prss8-S238A and Prss8-R44Q mice by testing the responses to pharmacological ENaC inhibition with triamterene. Upon administration of a single bolus of triamterene (10 μg g^{-1} bw), natriuresis over 6 h was similar in all genotypes suggesting normal baseline ENaC activity in mice expressing mutated prostasins (Fig. 5A). To test the effect of prolonged inhibition of ENaC-mediated sodium transport, we treated mice with a higher dose of triamterene given continuously in the drinking bottle (200 mg L^{-1}). This maneuver had previously been shown to induce salt wasting and hyperkalemia due to impaired ENaC-mediated sodium transport in mice lacking the serum-and glucocorticoid kinase 1 (SGK1) [29] or mTORC2 [28]. Daily triamterene intake was ~40 μg g^{-1} bw in all genotypes (Suppl. Fig. 5A) and was followed by increased diuresis and natriuresis as reflected by an increased urinary Na/K ratio and body weight loss on the 1st day (Fig. 5B, C). Thereafter, natriuresis and body weight loss stabilized in Prss8-wt and Prss8-S238A mice. In contrast, Prss8-R44Q continued to lose body weight and showed signs of massive dehydration, food and drinking avoidance (Fig 5E/F), leading to death or termination of the experiment in 75% of the animals (Fig. 5F). In Prss8-R44Q mice, we found signs of acute renal insufficiency such as azotemia, hyperkalemia, metabolic acidosis and hemoconcentration (Table 1). The plasma aldosterone concentration was massively increased, indicating a constellation consistent with an acquired type 1 pseudohypoaldosteronism (PHA1). In contrast, despite hyperaldosteronism Prss8-wt and Prss8-S238A mice did not develop signs of PHA1. Renal expression and urinary excretion of prostasin were not altered during triamterene treatment in all genotypes (Suppl. Fig. 6).

In addition to ENaC blockade, we also treated mice with furosemide and HCT with the drinking water. As shown in Fig. 5G, the diuretic effects of furosemide and HCT were similar in all genotypes. As expected, the diuretic effect of furosemide was stronger than that of HCT. Both diuretics moderately increased natriuresis in all genotypes (Fig. 5H). In contrast to the results with triamterene, treatment with furosemide and HCT was tolerated in all genotypes without salt wasting and major loss of body weight (Fig 5I, Suppl. Fig. 5).

Proteolytic activation of γ-ENaC is impaired in kidneys from Prss8-R44Q mice under triamterene treatment

We also analyzed tissue expression of ENaC subunits in kidneys from Prss8-wt, Prss8-S238A and Prss8-R44Q mice. In immunohistochemical analyses no differences regarding ENaC expression and its subcellular localization were detected in the three genotypes (Fig. 6). Under control conditions all three ENaC subunits were mainly localized in the cytosol. In all genotypes triamterene treatment appeared to increase overall expression of α-ENaC and enhanced the apical localization of all three ENaC subunits. These findings can be attributed to the increased plasma aldosterone levels due to the triamterene treatment (see Table 1) and are consistent with previous studies demonstrating the effects of low salt diet and chronic diuretic treatment on ENaC expression and apical targeting [30,31, 32]. In triamterene-treated

Prss8-R44Q mice, we observed tubular dilatation and atrophy, especially in ENaC-positive tubules, consistent with acute renal injury in these mice (Suppl. Fig 7). In all genotypes, triamterene crystalline nephropathy could be ruled out (data not shown).

In addition to immunohistochemistry, the protein expression of ENaC subunits and the proteolytic cleavage of the α- and γ-subunit were analyzed by Western blot. In kidney lysates, the expression of full-length (90 kDa) and furin-cleaved α-ENaC (25 kDa), β-ENaC (88 kDa) as well as full-length (72 kDa), furin-cleaved (61 kDa) and fully cleaved γ-ENaC (54 kDa) was similar in all genotypes under control conditions (Fig. 7). Under triamterene treatment, the expression of furin-cleaved α-ENaC increased significantly in all genotypes while the expression of β-ENaC was not altered in Prss8-wt and Prss8-R44Q mice, but increased in Prss8-S238A mice (Fig. 7A-D). In Prss8-wt and Prss8-S238A mice, expression of full-length γ-ENaC significantly decreased, whereas furin-cleaved and fully cleaved γ-ENaC was significantly increased (Fig. 8A/E-G). The expression of furin-cleaved and fully cleaved γ-ENaC did not increase to the same extent in Prss8-R44Q mice, suggesting impaired proteolytic ENaC activation. NCC and NKCC2 expression were not altered in Prss8-R44Q and Prss8-S238A mice under control diet and triamterene treatment, arguing against a compensatory role of either transporter (Suppl. Fig. 8).

Discussion

This study demonstrates that prostasin is involved in the stimulation of proteolytic ENaC activation both *in vitro* and *in vivo*. On a molecular level, proteolytic processing of prostasin at the R44 site appears to be more critical for proteolytic ENaC activation than its serine protease activity. This is evidenced by our *in vitro* finding that proteolytic ENaC activation by prostasin was fully preserved with the proteolytically inactive Prss8-S238A, consistent with previous reports[16,17], but was impaired with the zymogen-locked Prss8-R44Q. In contrast to Prss8-wt, expression of Prss8-S238A and Prss8-R44Q did not result in detectable prostasin-specific proteolytic activity at the cell surface. However, similar to Prss8-wt proteolytically inactive Prss8-S238A stimulated an endogenous protease as evidenced by the appearance of a substantial trypsin-like proteolytic activity at the cell surface. Importantly, a similar stimulatory effect was not observed with zymogen-locked prostasin Prss8-R44Q. Thus, impaired stimulation of an endogenous trypsin-like protease probably explains the incomplete proteolytic activation of ENaC by co-expressed Prss8-R44Q. Prostasin is known to be regulated by the transmembrane serine protease inhibitor, hepatocyte growth factor activator inhibitor (HAI)-2. A scavenging effect on protease inhibitors like HAI-2 is a possible mechanism to explain the stimulation of endogenous proteases by Prss8-wt or Prss8-S238A. Interestingly, unlike Prss8-wt and Prss8-S238A, the zymogen-locked Prss8-R44Q does not bind to HAI-2 [33]. Thus, an impaired activation of endogenous proteases by Prss8-R44Q may be due to its reduced ability to scavenge protease inhibitors. Alternatively, prostasin may recruit endogenous proteases to the plasma membrane by acting as a scaffold protein involved in trafficking. This scaffold function of prostasin may depend on its processing at the R44 activation site. The R44Q mutation prevents proteolytic conversion to a two-chain form that is encountered in Prss8-wt or Prss8-S238A after cleavage at R44. Therefore, Prss8-R44Q exists only in a single chain form with a different tertiary structure. However, the precise molecular mechanism involved in the prostasin mediated stimulation

of trypsin-like endogenous protease activity and the identity of the underlying proteases remain to be determined.

In vivo, Prss8-R44Q mice developed a pronounced compensatory hyperaldosteronism to adapt to low sodium diets, suggesting that dietary sodium restriction reveals a loss of function phenotype of Prss8-R44Q regarding its ability to mediate ENaC activation. This phenotype became even more apparent during continuous pharmacological ENaC inhibition by addition of triamterene to the drinking water without access to additional free water. In this setting, sodium- and water balance can only be maintained by development of diuretic tolerance which involves upregulation of the membrane expression of all ENaC subunits and cleavage of the α- and γ-subunit in Prss8-wt mice probably involving the stimulation of an additional endogenous protease (Fig. 7/8). These counterregulatory changes were preserved in Prss8-S238A mice, however, proteolytic activation of γ-ENaC was probably impaired in Prss8-R44Q mice which in turn led to volume depletion, dehydration, hyperkalemia and acidosis, consistent with acquired PHA1. This suggests that diuretic tolerance to triamterene requires Prss8-mediated proteolytic ENaC activation. The PHA1 phenotype of triamterene-treated Prss8-R44Q mice was similar to that of mice with an inducible deletion of γ-ENaC from the distal tubule [34]. These mice deteriorated rapidly within 1 to 2 days after deletion of γ-ENaC and stopped food and fluid intake. In addition, these mice developed massive hyperkalemia and acidosis which has been recently reported to be exacerbated by reduced ammonia generation during hyperkalemia [35].

ENaC-mediated sodium transport was not affected in the presence of the proteolytically inactive Prss8-S238A neither under control conditions nor under acute or continuous ENaC inhibition. This finding is in line with previous in vitro studies [21,22] and has been explained by the concept that the essential *in vivo* function of prostasin is sufficiently executed in the absence of its proteolytic activity [15], most likely through a scaffold function leading to recruitment and activation of other serine proteases as discussed above. In Fig. 8, we depict a model of how prostasin might mediate proteolytic ENaC activation in the distal nephron. Intracellular cleavage at the activation site R44 in Prss8-wt or Prss8-S238A probably induces a shift in the tertiary structure of prostasin that may enable the recruitment of another membrane-bound serine protease capable of activating ENaC by proteolysis, independent from the proteolytic activity of prostasin. In contrast, the scaffold function is probably impaired with Prss8-R44Q, hindering recruitment and proteolytic ENaC activation by other serine proteases.

At the transcript level Prss8 seems to be expressed in all cell types along the nephron including collecting duct principal cells [36-38]. Moreover, at the protein level its expression appears to be particularly prominent in distal tubular and collecting duct epithelial cells [15,16]. Thus, it is likely that ENaC and prostasin are co-expressed in the same cells which supports our conclusion that Prss8-R44Q leads to incomplete proteolytic ENaC activation *in vivo*. Nevertheless, we cannot rule out the possibility that replacing Prss8-wt with Prss8-R44Q has additional adverse effects on tubular function which may contribute to the observed triamterene intolerance in zymogen-locked Prss8-R44Q mice.

Our *in vivo* findings also indicate that the impaired function of Prss8-R44Q did not cause a compensatory upregulation of prostasin or matriptase. Indeed, expression of prostasin in the kidney was not altered in mice of all genotypes under control conditions, consistent with previous findings [15,16], and after ENaC blockade despite massive hyperaldosteronism. This latter finding is in agreement with a recent study reporting that prostasin was not up-regulated by aldosterone [39], in contrast to previous reports [12]. Moreover, the expression of matriptase, a membrane-bound serine protease activating prostasin [16,26], was similar in all genotypes.

The strength of this study lies in the investigation of mutant prostasin in the zymogen-locked (Prss8-R44Q) and proteolytically inactive state (Prss8-S238A) *in vitro* and *in vivo*. Of note, the results in both models were in good agreement. In mice lacking *prss8* in the colon, impaired colonic ENaC function has been reported to result in hyperaldosteronism and fecal sodium loss under low sodium diet [40]. It is tempting to speculate that mice lacking renal *prss8* would exhibit a lack of the prostasin scaffold function resulting in reduced proteolytic ENaC activation by an endogenous protease as observed in Prss8-R44Q mice. However, renal *prss8* ko mice would not allow to distinguish between effects due to proteolytic inactivity (as in Prss8-S238A) or resulting from the zymogen-locked state of prostasin (as in Prss8-R44Q) *in vivo*.

In conclusion, this study demonstrates that proteolytic ENaC activation was independent of the proteolytic activity of prostasin but impaired with zymogen-locked immature prostasin *in vitro* and *in vivo*. The results are compatible with an essential scaffold function of prostasin acting to recruit another serine protease for proteolytic ENaC activation.

Materials and methods

cDNA clones

Full-length cDNAs for murine α-, β-, and γ-ENaC were kindly provided by M. Mall (Heidelberg, Germany). Full-length cDNA for murine Prss8-wt was kindly provided by E. Hummler (Lausanne, Switzerland). cDNAs were subcloned into the pTLN vector [41]. Linearized plasmids were used as templates for cRNA synthesis using T7 RNA polymerases (mMessage mMachine, Ambion, Austin, TX, USA). Single-point mutations in Prss8 (Prss8-S238A, Prss8-R44Q) were generated using QuikChange Lightening site-directed mutagenesis kit (Agilent Technologies, Waldbronn, Germany). Sequences were confirmed by sequence analysis (LGC Genomics, Berlin, Germany).

Isolation of oocytes and two-electrode voltage-clamp experiments

Isolation of oocytes and two-electrode voltage-clamp experiments were performed essentially as described previously [4,7,42]. Defolliculated stage V-VI oocytes were obtained from ovarian lobes of adult female *Xenopus laevis* in accordance with the principles of German legislation, with approval by the animal welfare officer for the University of Erlangen-Nürnberg, and under the governance of the state veterinary health inspectorate (approval number Az. 55.2-2532-2-527). Animals were anesthetized in 0.2 % MS222 (Sigma, Taufkirchen, Germany) and ovarian lobes were obtained by a small abdominal

incision. Oocytes were injected with cRNAs encoding the three subunits (α, β, γ) of mouse ENaC (0.02 ng/β/oocyte). The co-injected amount of cRNA for mouse Prss8-WT, Prss8-S238A or Prss8-R44Q was 2 ng per oocyte. To prevent Na^+ overloading of oocytes, injected oocytes were maintained in a low sodium ND9 solution (in mM: 9 NaCl, 2 KCl, 87 N-methyl-D-glutamine-Cl, 1.8 $CaCl_2$, 1 $MgCl_2$, 5 HEPES, pH 7.4 adjusted with Tris) supplemented with 100 units/ml sodium penicillin and 100 μg mL^{-1} streptomycin sulphate. Oocytes were studied 48 hours after cRNA injection. ENaC-mediated whole-cell currents (ΔI_{ami}) were determined at a holding potential of −60 mV by washing out amiloride (2 μM, Sigma-Aldrich, Taufkirchen, Germany) with amiloride-free bath solution and subtracting the whole-cell currents measured in the presence of amiloride from the corresponding whole-cell currents recorded in the absence of amiloride. Modified ND96 solution was used as standard bath solution (in mM: 96 NaCl, 4 KCl, 1 $CaCl_2$, 1 $MgCl_2$, 10 HEPES, pH 7.4 adjusted with Tris). To evaluate the degree of proteolytic ENaC activation, α-chymotrypsin type II from bovine pancreas (Sigma-Aldrich, Taufkirchen, Germany) was applied in a concentration of 2 μg mL^{-1} in ND96 solution. In this concentration the prototypical protease chymotrypsin causes complete proteolytic ENaC activation in the oocyte expression system [4,42].

Detection of Prss8 at the cell surface using a biotinylation approach

To separate cell surface expressed Prss8 from intracellular Prss8, cell surface proteins were labeled with biotin essentially as described previously [4,7,43-45]. Biotinylated cell surface proteins and intracellular proteins were studied by Western blot analysis under reducing conditions. Mouse Prss8 was detected using mouse anti-human Prss8 (BD Transduction Laboratories, catalog no. 612173) at a dilution of 1:250 and a secondary horseradish peroxidase-labeled goat anti-mouse antibody (Abcam, catalog no. ab97023) at a dilution of 1:50,000. To validate separation of cell surface proteins from intracellular proteins by biotinylation, blots were stripped and re-probed using a α-tubulin antibody (Invitrogen, catalog no. 62204) at a dilution of 1:2,000.

Determination of surface-bound proteolytic activity of oocytes

Proteolytic activity was quantified using the fluorogenic substrate Boc-Gln-Ala-Arg-AMC (Boc-QAR-AMC) (Boc: t-Butyloxycarbonyl; AMC: 7-Amino-4-methylcoumarin; R&D systems, Abingdon, UK) or Ac-Lys-His-Tyr-Arg-AMC (Ac: Acetyl; KareBay Biochem Inc., Monmouth Junction, NJ, USA). The experimental protocol was similar to that described by Reihill et al. [24]. Boc-QAR-AMC detects the activity of a wide range of trypsin-like proteases[25], whereas Ac-KHYR-AMC has been reported to be an optimal prostasin substrate [23]. Each individual oocyte was placed into a well of a 96-well plate containing 100 μl of standard ND9 solution supplemented with 10 μM fluorogenic substrate. The fluorescence signal resulting from substrate hydrolysis at the cell surface was continuously recorded over a time period up to 190 min using a TECAN plate reader (360 nm excitation/465 nm emission wavelength).

Mouse studies

Experiments were performed on 3-month-old genetically modified knockin mice carrying mutations of the prostasin gene that resulted either in enzymatically inactive (Prss8-S238A

[15]) or zymogen-locked prostasin (Prss8-R44Q [16]). Prss8-wildtype littermate mice served as controls. Imported Prss8-S238A and Prss8-R44Q mice on a mixed background were backcrossed onto a 129 S1/SvImJ background. Genotyping was done using PCR. Mice were kept on a 12:12-h light-dark cycle and fed a standard chow (ssniff, V1534, Soest, Germany) with tap water ad libitum.

In healthy Prss8-wt, Prss8-S238A and Prss8-R44Q mice, renal sodium handling was studied in metabolic cages. Mice were kept for 2 days on a control diet (C1000, sodium and potassium content 110 μmol·g^{-1} and 178 μmol g^{-1}, respectively, Altromin, Lage, Germany) followed by 5 days of low sodium diet (C1036, sodium and potassium content 10 μmol·g^{-1} and 178 μmol g^{-1}) with or without high potassium (1 tablet Kalinor™ dissolved in 400ml drinking water, final concentration 100 mM). To investigate the responses to diuretics, mice were maintained in metabolic cages and treated for 4 days with the ENaC inhibitor triamterene (200 mg L^{-1} in the drinking water at pH 3), the NKCC2 inhibitor furosemide (125 mg L^{-1} in the drinking water) or the NCC inhibitor hydrochlorothiazide (400 mg L^{-1} in the drinking water) as described in previous studies [28,29]. Acute responses to triamterene or vehicle (5% DMSO, pH 3) were studied by bolus administration of 10 μg g^{-1} i.p. and subsequent collection of urine for 6 h.

All mouse experiments were conducted according to the National Institutes of Health Guide for the Care and Use of Laboratory Animals and the German law for the welfare of animals, and they were approved by local authorities (Regierungspraesidium Tuebingen, approval number M6/17).

Laboratory measurements

Urinary creatinine was measured with a colorimetric Jaffé assay (Labor+Technik, Berlin, Germany), urinary sodium and potassium concentration as well as fecal sodium content (after dissolution in nitric acid) with flame photometry (Eppendorf EFUX 5057, Hamburg, Germany). 24 h urinary sodium and potassium excretion was normalized to body weight. Plasma urea was measured enzymatically using a colorimetric assay (Labor+Technik, Berlin, Germany), plasma aldosterone and urinary prostasin excretion were measured using ELISA kits (IBL, Hamburg, Germany, and Abcam, Cambridge, UK respectively). Plasma sodium and potassium were measured using an IL GEM® Premier 3000 blood gas analyzer (Instrumentation Laboratory, Munich, Germany).

Western blot from kidney tissue of mice

Western blot analysis of prostasin, ENaC subunits as well as NaCl-contransporter (NCC) and Na-K-Cl cotransporter (NKCC2) was performed from a membrane protein preparation of kidney cortex collected under control condition or 24 h after continuous triamterene treatment. Half the kidney per mouse was sliced, and the cortex was dissected using a scalpel. Homogenization was performed using a Dounce homogenizer in 1 ml lysis buffer containing 250 mM sucrose, 10 mM triethanolamine HCl, 1.6 mM ethanolamine and 0.5 EDTA at pH 7.4 (all Sigma) [46,47]. During all preparation steps, aprotinin (40 μg ml^{-1}) and a protease inhibitor cocktail (final concentration 0.1 x stock; mini-complete, Roche) was present to avoid ENaC cleavage *in vitro*. Homogenates were centrifuged at 1,000 g for

removal of the nuclei. Subsequently, the supernatant was centrifuged at 20,000 g for 30 min at 4°C, and the resulting pellet containing plasma membranes was resuspended and diluted to a concentration of 5 mg·L^{-1}. Native samples were boiled in Laemmli buffer at 70°C for 10 min. For analysis of γ-ENaC cleavage fragments, samples were deglycosylated using PNGaseF according to the manufacturer's instructions (NEB, Ipswich, USA). A similar strategy has recently been used to improve the detection of fully cleaved γ-ENaC in rodent kidney [8]. First, samples were denatured with a glycoprotein denaturing buffer. Samples were then incubated with glycobuffer, NP-40 and PNGaseF for 1h at 37°C. Subsequently, 20 μg of sample was loaded on an 8%-polyacrylamide gel for SDS-PAGE of prostasin and ENaC subunits or on a 4-15% gradient for SDS-PAGE of NCC and NKCC2. Thereafter, proteins were blotted onto a nitrocellulose membrane (Amersham GE healthcare) and probed for the target protein using primary antibodies outlined below. Recombinant murine prostasin was used as a positive control (amino acids 30-289, R&D systems). Signals were detected using fluorescent secondary antibody labelled with IRDye 800CW or IRDye 680CW and a fluorescence scanner (Licor Odyssey, Lincoln, USA). For loading control, total protein was measured using Revert Total Protein Stain (Licor, Lincoln, USA).

Immunohistochemistry

For analysis of tissue expression of ENaC subunits, kidneys were collected under control condition or 2 days after continuous triamterene treatment. Paraffin-embedded formalin-fixed sections (2 μm) were deparaffinized and rehydrated using standard protocols. Antigen retrieval was accomplished after heating for 2.5 min in antigen retrieval solution pH 6.1 (DAKO Deutschland GmbH, Hamburg, Germany) using a pressure cooker (NxGen DC-Modul, Zytomed, Berlin, Germany). Kidney sections were blocked for 15 minutes with normal goat serum diluted 1:5 in 50 mM tris(hydroxymethyl)-aminomethane (Tris), pH 7.4, supplemented with 1% (w/v) skim milk (Bio-Rad Laboratories, Munich, Germany), followed by overnight incubation at 4°C with the same antibodies as used in Western blot (polyclonal rabbit anti-α-ENaC 1:100; polyclonal rabbit anti-β-ENaC 1:1000; anti-γ-ENaC 1:500) and subsequent washing in Tris buffer (50 mM Tris, pH 7.4, supplemented with 0.05% (v/v) Tween 20 (Sigma-Aldrich, Munich, Germany; 3 x 5 minutes). The secondary antibody (a biotinylated goat anti-rabbit, Vector Laboratories, Burlingame, CA USA; 1:500) was applied for 30 minutes at room temperature. Sections were further processed using the VectaStain ABC kit according to the manufacturer's instructions and DABImmpact (both Vector Laboratories) as substrate. Finally, the sections were counterstained in hemalaun, dehydrated, and mounted for observation using an Olympus Bx60 upright microscope.

Primary Antibodies used in mouse samples

Antibodies against murine α- and β-ENaC were raised in rabbits against the amino acids 45-68 for α-ENaC and 617-638 for β-ENaC using a commercial service (Pineda, Berlin, Germany). Anti-γ-ENaC was purchased from Stressmarq (SPC-405, Viktoria, Canada). This antibody had been raised in rabbits against the C-terminal amino acids 634–655 of γ-ENaC. All ENaC antibodies were based on the peptide sequences first introduced and validated by Masilamani et al. [48]. The antibodies against α- and β-ENaC had been affinity-purified while anti-γ-ENaC had been purified with protein A according to the manufacturer. Commercially available polyclonal antibodies were used to probe NCC (SPC-402, Stressmarq), NKCC2

(SPC-401, Stressmarq), prostasin (15527-1-AP, proteintech) and matriptase (AF3946, R&D systems).

Statistical analysis

Data are provided as means with SEM. Data were tested for normality with the Kolmogorov-Smirnov-Test, D'Agostino and Pearson omnibus normality test and Shapiro-Wilk-Test. Variances were tested using the Bartlett's test for equal variances. Accordingly, data were tested for significance with parametric or nonparametric ANOVA followed by Bonferroni, Dunnett's, Dunn's, or Tukey's Multiple Comparison *posthoc* test, paired or unpaired Student's t-test, or Mann-Whitney U-test where applicable using GraphPad Prism 8, GraphPad Software (San Diego, CA, www.graphpad.com). Densitometric analysis of Western blots was done using Image Studio Version 3.1.4 (Licor). A p value <0.05 at two-tailed testing was considered statistically significant.

Supplementary Material

Refer to Web version on PubMed Central for supplementary material.

Acknowledgments

This study was supported by grants from the Deutsche Forschungsgemeinschaft (DFG, German Research Foundation) to FA (AR 1092/2-2) and CK/KA/CD (project number 387509280, SFB 1350, subprojects A4 to CK and C2 to KA/CD), by a grant from IZKF Tübingen to DE and in part by the Intramural Research Program of the NIH, NIDCR (RS, THB).

We acknowledge the artwork in Figure 9 by Hao Tian and the technical support by Andrea Janessa.

References

1. Rossier BC, Stutts MJ. Activation of the epithelial sodium channel (ENaC) by serine proteases. Annual review of physiology. 2009;71:361–379.
2. Kleyman TR, Kashlan OB, Hughey RP. Epithelial Na(+) Channel Regulation by Extracellular and Intracellular Factors. Annu Rev Physiol. 2018;80:263–281. [PubMed: 29120692]
3. Kleyman TR, Carattino MD, Hughey RP. ENaC at the cutting edge: regulation of epithelial sodium channels by proteases. J Biol Chem. 2009;284(31):20447–20451. [PubMed: 19401469]
4. Diakov A, Bera K, Mokrushina M, Krueger B, Korbmacher C. Cleavage in the {gamma}-subunit of the epithelial sodium channel (ENaC) plays an important role in the proteolytic activation of near-silent channels. The Journal of physiology. 2008;586(Pt 19):4587–4608. [PubMed: 18669538]
5. Haerteis S, Krappitz A, Krappitz M, et al. Proteolytic activation of the human epithelial sodium channel by trypsin IV and trypsin I involves distinct cleavage sites. The Journal of biological chemistry. 2014;289(27):19067–19078. [PubMed: 24841206]
6. Haerteis S, Schork A, Dörffel T, et al. Plasma kallikrein activates the epithelial sodium channel (ENaC) in vitro but is not essential for volume retention in nephrotic mice. Acta physiologica (Oxford, England). 2018;224(1):e13060.
7. Haerteis S, Krappitz M, Diakov A, Krappitz A, Rauh R, Korbmacher C. Plasmin and chymotrypsin have distinct preferences for channel activating cleavage sites in the gamma subunit of the human epithelial sodium channel. The Journal of general physiology. 2012;140(4):375–389. [PubMed: 22966015]
8. Frindt G, Shi S, Kleyman TR, Palmer LG. Cleavage state of γENaC in mouse and rat kidney. Am J Physiol Renal Physiol. 2021.

9. Vuagniaux G, Vallet V, Jaeger NF, et al. Activation of the amiloride-sensitive epithelial sodium channel by the serine protease mCAP1 expressed in a mouse cortical collecting duct cell line. J Am Soc Nephrol. 2000;11(5):828–834. [PubMed: 10770960]
10. Adachi M, Kitamura K, Miyoshi T, et al. Activation of epithelial sodium channels by prostasin in Xenopus oocytes. J Am Soc Nephrol. 2001;12(6):1114–1121. [PubMed: 11373334]
11. Bruns JB, Carattino MD, Sheng S, et al. Epithelial Na+ channels are fully activated by furin- and prostasin-dependent release of an inhibitory peptide from the gamma-subunit. J Biol Chem. 2007;282(9):6153–6160. [PubMed: 17199078]
12. Narikiyo T, Kitamura K, Adachi M, et al. Regulation of prostasin by aldosterone in the kidney. The Journal of clinical investigation. 2002;109(3):401–408. [PubMed: 11828000]
13. Andersen H, Friis UG, Hansen PB, Svenningsen P, Henriksen JE, Jensen BL. Diabetic nephropathy is associated with increased urine excretion of proteases plasmin, prostasin and urokinase and activation of amiloride-sensitive current in collecting duct cells. Nephrology, dialysis, transplantation : official publication of the European Dialysis and Transplant Association - European Renal Association. 2015;30(5):781–789.
14. Zachar R, Jensen BL, Svenningsen P. Dietary Na(+) intake in healthy humans changes the urine extracellular vesicle prostasin abundance while the vesicle excretion rate, NCC, and ENaC are not altered. Am J Physiol Renal Physiol. 2019;317(6):F1612–f1622. [PubMed: 31566425]
15. Peters DE, Szabo R, Friis S, et al. The membrane-anchored serine protease prostasin (CAP1/PRSS8) supports epidermal development and postnatal homeostasis independent of its enzymatic activity. J Biol Chem. 2014;289(21):14740–14749. [PubMed: 24706745]
16. Friis S, Madsen DH, Bugge TH. Distinct Developmental Functions of Prostasin (CAP1/PRSS8) Zymogen and Activated Prostasin. J Biol Chem. 2016;291(6):2577–2582. [PubMed: 26719335]
17. Yu JX, Chao L, Chao J. Prostasin is a novel human serine proteinase from seminal fluid. Purification, tissue distribution, and localization in prostate gland. J Biol Chem. 1994;269(29):18843–18848. [PubMed: 8034638]
18. Hummler E, Dousse A, Rieder A, et al. The channel-activating protease CAP1/Prss8 is required for placental labyrinth maturation. PloS one. 2013;8(2):e55796. [PubMed: 23405214]
19. Leyvraz C, Charles RP, Rubera I, et al. The epidermal barrier function is dependent on the serine protease CAP1/Prss8. J Cell Biol. 2005;170(3):487–496. [PubMed: 16061697]
20. Yu JX, Chao L, Chao J. Molecular cloning, tissue-specific expression, and cellular localization of human prostasin mRNA. J Biol Chem. 1995;270(22):13483–13489. [PubMed: 7768952]
21. Andreasen D, Vuagniaux G, Fowler-Jaeger N, Hummler E, Rossier BC. Activation of epithelial sodium channels by mouse channel activating proteases (mCAP) expressed in Xenopus oocytes requires catalytic activity of mCAP3 and mCAP2 but not mCAP1. J Am Soc Nephrol. 2006;17(4):968–976. [PubMed: 16524950]
22. Carattino MD, Mueller GM, Palmer LG, et al. Prostasin interacts with the epithelial Na+ channel and facilitates cleavage of the γ-subunit by a second protease. Am J Physiol Renal Physiol. 2014;307(9):F1080–1087. [PubMed: 25209858]
23. Shipway A, Danahay H, Williams JA, Tully DC, Backes BJ, Harris JL. Biochemical characterization of prostasin, a channel activating protease. Biochemical and biophysical research communications. 2004;324(2):953–963. [PubMed: 15474520]
24. Reihill JA, Walker B, Hamilton RA, et al. Inhibition of Protease-Epithelial Sodium Channel Signaling Improves Mucociliary Function in Cystic Fibrosis Airways. American journal of respiratory and critical care medicine. 2016;194(6):701–710. [PubMed: 27014936]
25. Kawabata S, Miura T, Morita T, et al. Highly sensitive peptide-4-methylcoumaryl-7-amide substrates for blood-clotting proteases and trypsin. Eur J Biochem. 1988;172(1):17–25. [PubMed: 3278905]
26. Netzel-Arnett S, Currie BM, Szabo R, et al. Evidence for a matriptase-prostasin proteolytic cascade regulating terminal epidermal differentiation. J Biol Chem. 2006;281(44):32941–32945. [PubMed: 16980306]
27. Wörn M, Bohnert BN, Alenazi F, et al. Proteasuria in nephrotic syndrome-quantification and proteomic profiling. J Proteomics. 2020:103981. [PubMed: 32927112]

28. Grahammer F, Nesterov V, Ahmed A, et al. mTORC2 critically regulates renal potassium handling. J Clin Invest. 2016;126(5):1773–1782. [PubMed: 27043284]
29. Artunc F, Ebrahim A, Siraskar B, et al. Responses to diuretic treatment in gene-targeted mice lacking serum- and glucocorticoid-inducible kinase 1. Kidney & blood pressure research. 2009;32(2):119–127. [PubMed: 19401625]
30. Nesterov V, Krueger B, Bertog M, Dahlmann A, Palmisano R, Korbmacher C. In Liddle Syndrome, Epithelial Sodium Channel Is Hyperactive Mainly in the Early Part of the Aldosterone-Sensitive Distal Nephron. Hypertension. 2016;67(6):1256–1262. [PubMed: 27170740]
31. Loffing J, Pietri L, Aregger F, et al. Differential subcellular localization of ENaC subunits in mouse kidney in response to high- and low-Na diets. Am J Physiol Renal Physiol. 2000;279(2):F252–258. [PubMed: 10919843]
32. Kim GH. Long-term adaptation of renal ion transporters to chronic diuretic treatment. American journal of nephrology. 2004;24(6):595–605. [PubMed: 15564765]
33. Szabo R, Bugge TH. Loss of HAI-2 in mice with decreased prostasin activity leads to an early-onset intestinal failure resembling congenital tufting enteropathy. PloS one. 2018;13(4):e0194660. [PubMed: 29617460]
34. Boscardin E, Perrier R, Sergi C, et al. Plasma Potassium Determines NCC Abundance in Adult Kidney-Specific gammaENaC Knockout. J Am Soc Nephrol. 2018.
35. Harris AN, Grimm PR, Lee H-W, et al. Mechanism of Hyperkalemia-Induced Metabolic Acidosis. Journal of the American Society of Nephrology. 2018;29(5):1411–1425. [PubMed: 29483157]
36. Park J, Shrestha R, Qiu C, et al. Single-cell transcriptomics of the mouse kidney reveals potential cellular targets of kidney disease. Science. 2018;360(6390):758–763. [PubMed: 29622724]
37. Chen L, Lee JW, Chou CL, et al. Transcriptomes of major renal collecting duct cell types in mouse identified by single-cell RNA-seq. Proceedings of the National Academy of Sciences of the United States of America. 2017;114(46):E9989–e9998. [PubMed: 29089413]
38. Lee JW, Chou CL, Knepper MA. Deep Sequencing in Microdissected Renal Tubules Identifies Nephron Segment-Specific Transcriptomes. J Am Soc Nephrol. 2015;26(11):2669–2677. [PubMed: 25817355]
39. Oxlund C, Kurt B, Schwarzensteiner I, et al. Albuminuria is associated with an increased prostasin in urine while aldosterone has no direct effect on urine and kidney tissue abundance of prostasin. Pflugers Arch. 2017;469(5-6):655–667. [PubMed: 28233126]
40. Malsure S, Wang Q, Charles RP, et al. Colon-specific deletion of epithelial sodium channel causes sodium loss and aldosterone resistance. J Am Soc Nephrol. 2014;25(7):1453–1464. [PubMed: 24480829]
41. Lorenz C, Pusch M, Jentsch TJ. Heteromultimeric CLC chloride channels with novel properties. Proceedings of the National Academy of Sciences of the United States of America. 1996;93(23):13362–13366. [PubMed: 8917596]
42. Ilyaskin AV, Diakov A, Korbmacher C, Haerteis S. Activation of the Human Epithelial Sodium Channel (ENaC) by Bile Acids Involves the Degenerin Site. J Biol Chem. 2016;291(38):19835–19847. [PubMed: 27489102]
43. Bohnert BN, Daiminger S, Worn M, et al. Urokinase-type plasminogen activator (uPA) is not essential for epithelial sodium channel (ENaC)-mediated sodium retention in experimental nephrotic syndrome. Acta physiologica (Oxford, England). 2019;227(4):e13286.
44. Krueger B, Yang L, Korbmacher C, Rauh R. The phosphorylation site T613 in the beta-subunit of rat epithelial Na(+) channel (ENaC) modulates channel inhibition by Nedd4-2. Pflugers Arch. 2018;470(4):649–660. [PubMed: 29397423]
45. Ilyaskin AV, Korbmacher C, Diakov A. Inhibition of the epithelial sodium channel (ENaC) by connexin 30 involves stimulation of clathrin-mediated endocytosis. J Biol Chem. 2021:100404. [PubMed: 33577799]
46. Yang L, Frindt G, Lang F, Kuhl D, Vallon V, Palmer LG. SGK1-dependent ENaC processing and trafficking in mice with high dietary K intake and elevated aldosterone. Am J Physiol Renal Physiol. 2017;312(1):F65–f76. [PubMed: 27413200]

47. Xiao M, Bohnert BN, Aypek H, et al. Plasminogen deficiency does not prevent sodium retention in a genetic mouse model of experimental nephrotic syndrome. Acta physiologica (Oxford, England). 2020:e13512.

48. Masilamani S, Kim GH, Mitchell C, Wade JB, Knepper MA. Aldosterone-mediated regulation of ENaC alpha, beta, and gamma subunit proteins in rat kidney. J Clin Invest. 1999;104.

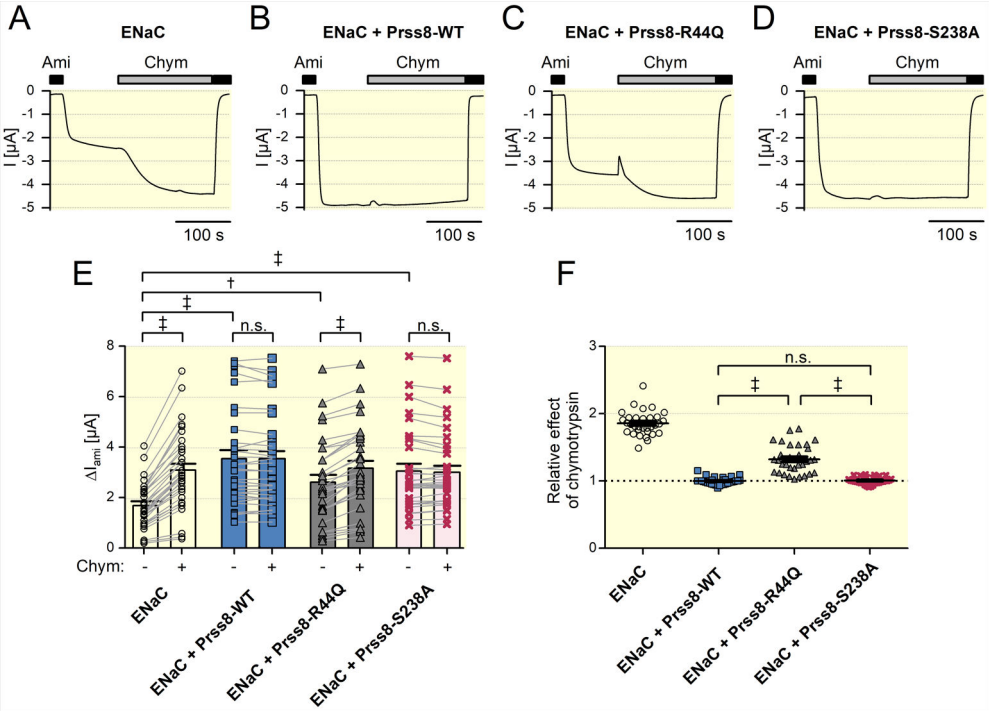

Figure 1: Co-expression of zymogen-locked Prss8-R44Q stimulates ENaC currents to a lesser extent than wild-type Prss8 or proteolytically inactive Prss8-S238A

A-D Representative whole-cell current traces recorded in an oocyte expressing murine ENaC alone (ENaC; A) or in combination with murine wild-type Prss8 (ENaC + Prss8-WT; B), zymogen-locked Prss8-R44Q (ENaC + Prss8-R44Q; C), or catalytically inactive Prss8-S238A (ENaC + Prss8-S238A; D). Presence of amiloride (Ami, 2 μM) or chymotrypsin (Chym, 2 μg/ml) in the bath solution is indicated by corresponding black or grey bars, respectively.

E Summary of data obtained in similar experiments as in A-D. Individual and mean ± SEM values of ΔI_{ami} before (−) and after (+) application of chymotrypsin. Measurements performed in the same oocyte are connected by a line (n=32 from 4 different batches of oocytes). ‡, $p<0.001$; †, $p<0.01$; n.s. not significant; Student's *t* test.

F Summary of the data shown in E normalized as relative stimulatory effect of chymotrypsin on ΔI_{ami}, i.e. the ratio of ΔI_{ami} after chymotrypsin to ΔI_{ami} before chymotrypsin. Thus, a ratio of one (dotted line) indicates the absence of a stimulatory effect of chymotrypsin on ENaC. Individual and mean ± SEM values are shown. ‡, $p<0.001$; n.s. not significant; one-way ANOVA with Bonferroni post hoc test.

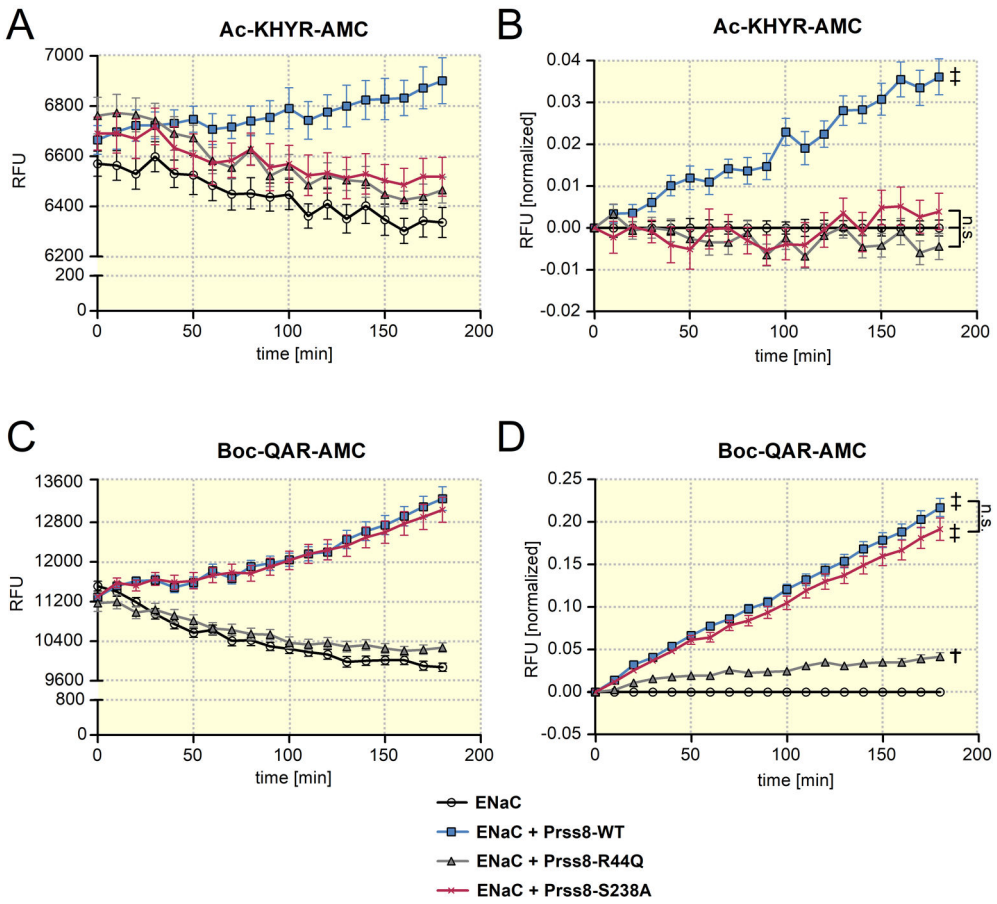

Figure 2: Analysis of protease activity at the cell surface of oocytes expressing wild-type Prss8, zymogen-locked Prss8-R44Q or catalytically inactive Prss8-S238A.

Proteolytic activity of prostasin (A, B) or of trypsin-like proteases (C, D) at the cell surface of oocytes detected using Ac-KHYR-AMC or Boc-QAR-AMC fluorogenic substrate, respectively. Progress curves of proteolytic activity (mean ± SEM) are shown for oocytes expressing ENaC alone or co-expressing ENaC with Prss8-wt, Prss8-R44Q or Prss8-S238A. In A and C, representative recordings of absolute fluorescent signal values (RFU=relative fluorescent unit) obtained in oocytes from one batch are shown (A: n=8; C: n=10). In B and D, RFU values obtained in different batches of oocytes (B: n=40, N=5; D: n=78, N=9) were normalized to account for the batch to batch variability of the absolute RFU values and to correct for the signal decline due to photobleaching. In each individual recording RFU values were normalized to the initial RFU value at the beginning of the measurement. In addition, for each time point the average normalized RFU values measured in oocytes expressing ENaC alone were subtracted from the corresponding individual normalized RFU values. ‡, $p<0.001$; †, $p<0.01$; n.s., not significant; one-way ANOVA with Bonferroni post hoc test (at the time point 180 min).

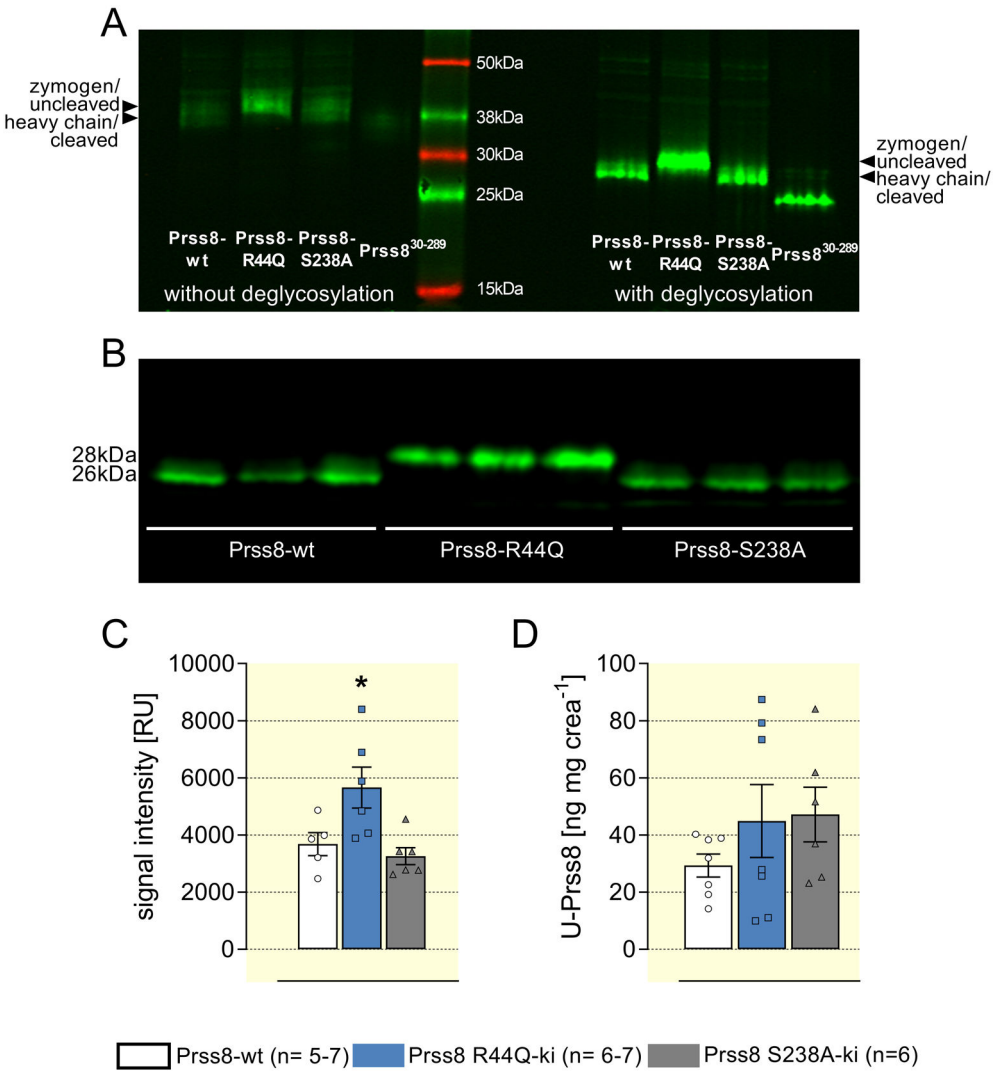

Figure 3. Renal expression and urinary excretion of prostasin in Prss8-wt, Prss8-S238A and Prss8-R44Q mutant mice

A Western blot appearance of wild-type and mutant prostasin in kidney tissue as well as a recombinant truncated murine prostasin (amino acids 30-289, predicted mass 28 kDa) with or without deglycosylation by PNGaseF. Note that deglycosylation leads to single clear bands, compatible with glycosylation of prostasin in vivo.

B Expression of prostasin as analyzed by Western blot from kidney lysates treated with PNGaseF for deglycosylation. Representative lanes with n=3 for each genotype.

C Densitometric analysis of the obtained bands from two Western blots with n=5-6 for each genotype.

D Urinary excretion of prostasin measured with an ELISA in 24 h urine samples.

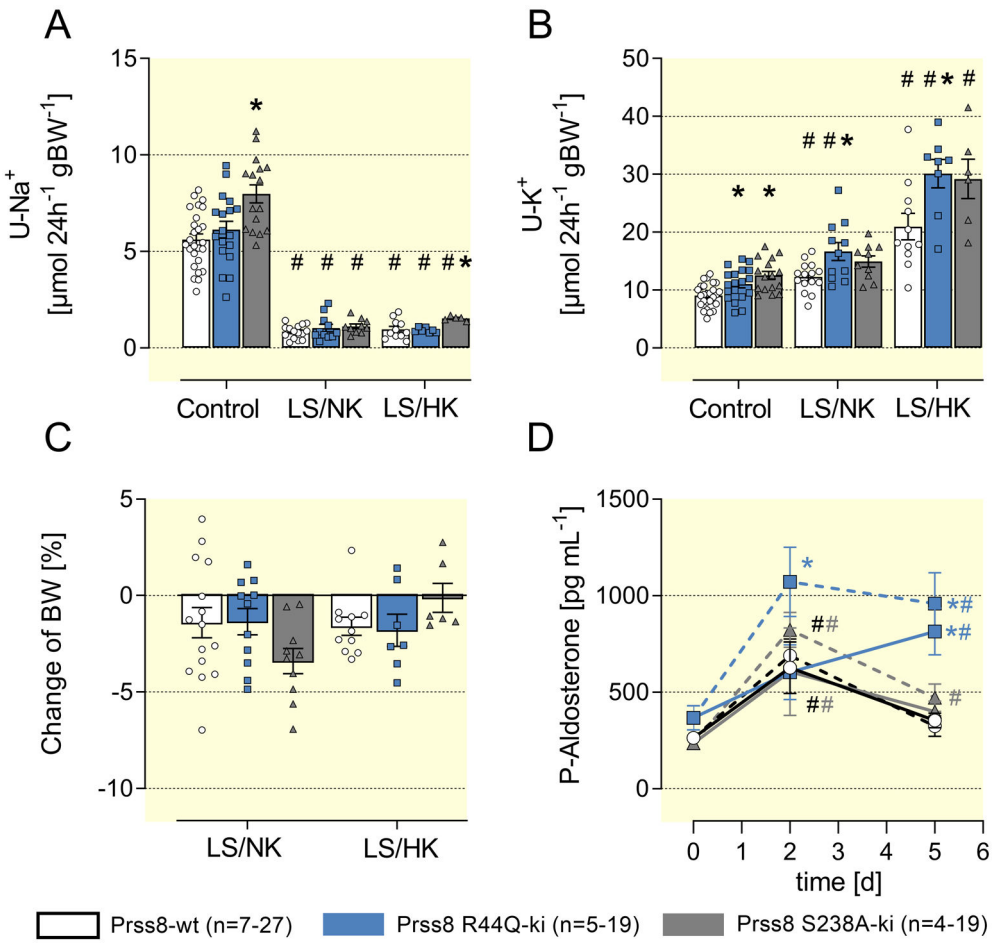

Figure 4: Sodium conservation is not impaired in Prss8-wt, Prss8-S238A and Prss8-R44Q mutant mice

(A, B) 24 h urinary sodium and potassium excretion under a control, low sodium (LS/NK) or low sodium + high potassium diet (LS/HK) on the 5th day.

(C) Change in body weight calculated as the difference between baseline and value on the 5th day.

(D) Time course of plasma aldosterone concentration after switch to a low sodium diet with normal potassium content (LS/NK, solid lines) or a low sodium with a high potassium content (LS/HK, dashed lines).

# indicates significant difference between low sodium and control diet, * indicates significant difference between the genotypes

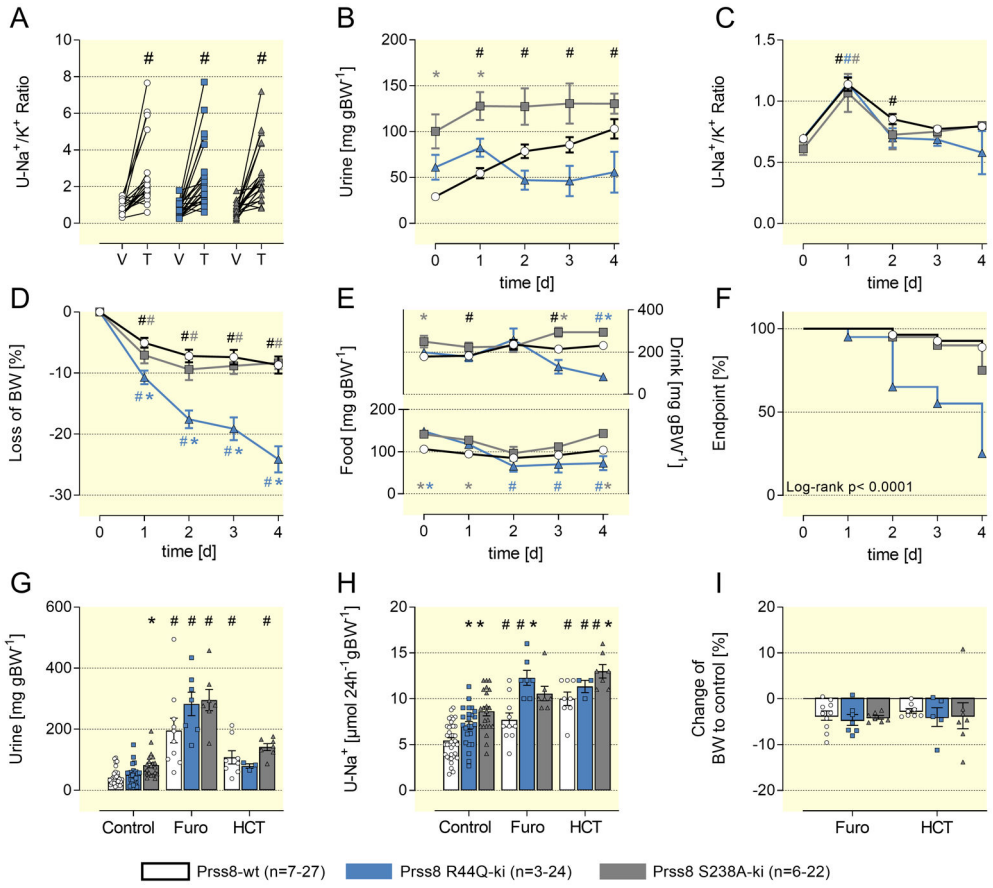

Figure 5: Effect of diuretics in Prss8-S238A and Prss8-R44Q mutant mice

A Natriuretic response expressed as urinary Na/K ratio to the acute administration of vehicle (V, injectable water, 5µL g^{-1}) or the ENaC inhibitor triamterene (T, 10 µg g^{-1}). Urine was collected for 6 hours.

B, C Effect of a four day treatment with the ENaC inhibitor triamterene on urine output and urinary sodium/potassium ratio.

D, E Course of body weight as well as fluid and food intake during triamterene treatment.

F Kaplan-Meier curve for the probability to reaching the end point weight loss greater than 25% of the baseline value which prompted termination of the experiment and euthanasia in that particular mice.

G-I Effect of a four day treatment with the NKCC2 inhibitor furosemide or the NCC inhibitor HCT on urine output, natriuresis and body weight.

abbreviations: C control, V vehicle, T triamterene, Furo furosemide, HCT hydrochlorothiazide

# indicates significant difference between control and diuretic treatment, * indicates significant difference between the genotypes

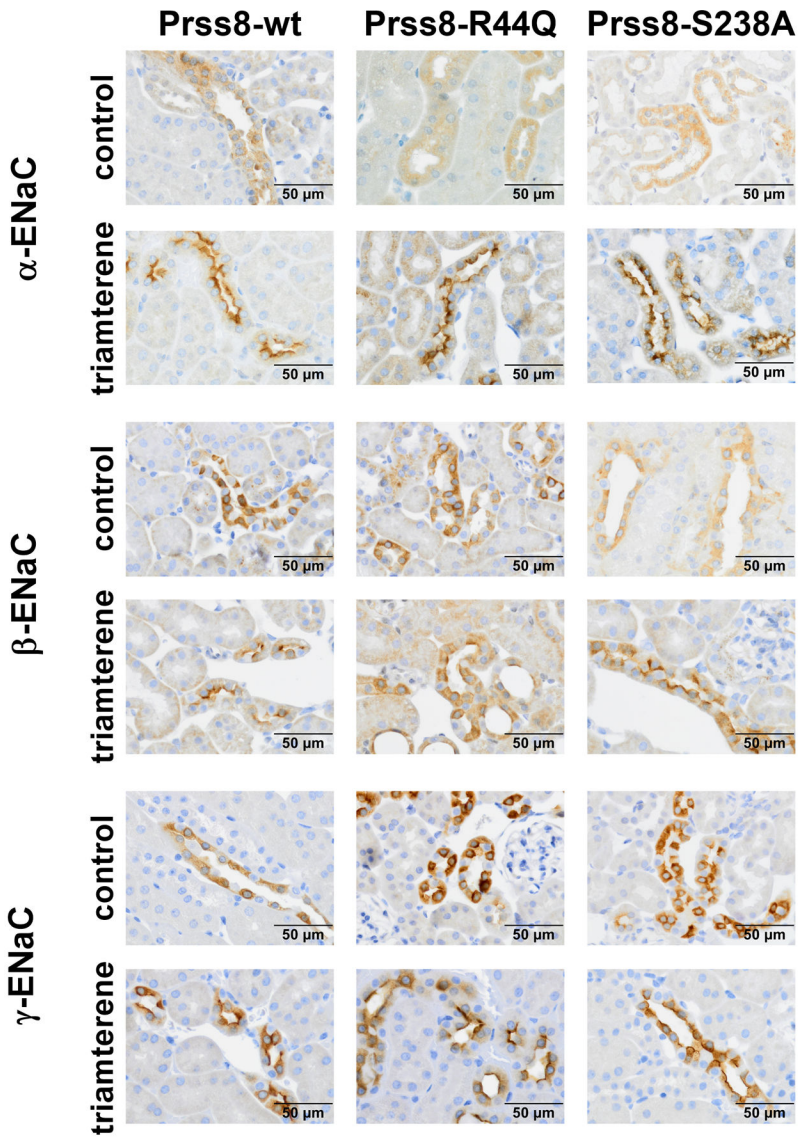

Figure 6: Tissue expression of ENaC subunits in kidneys from Prss8-wt, Prss8-S238A and Prss8-R44Q mutant mice under control and triamterene treatment

Immunohistochemical staining of fixed kidney tissue. In all genotypes, there is increased abundance of the α-subunit and apical staining for all subunits after a two day triamterene treatment.

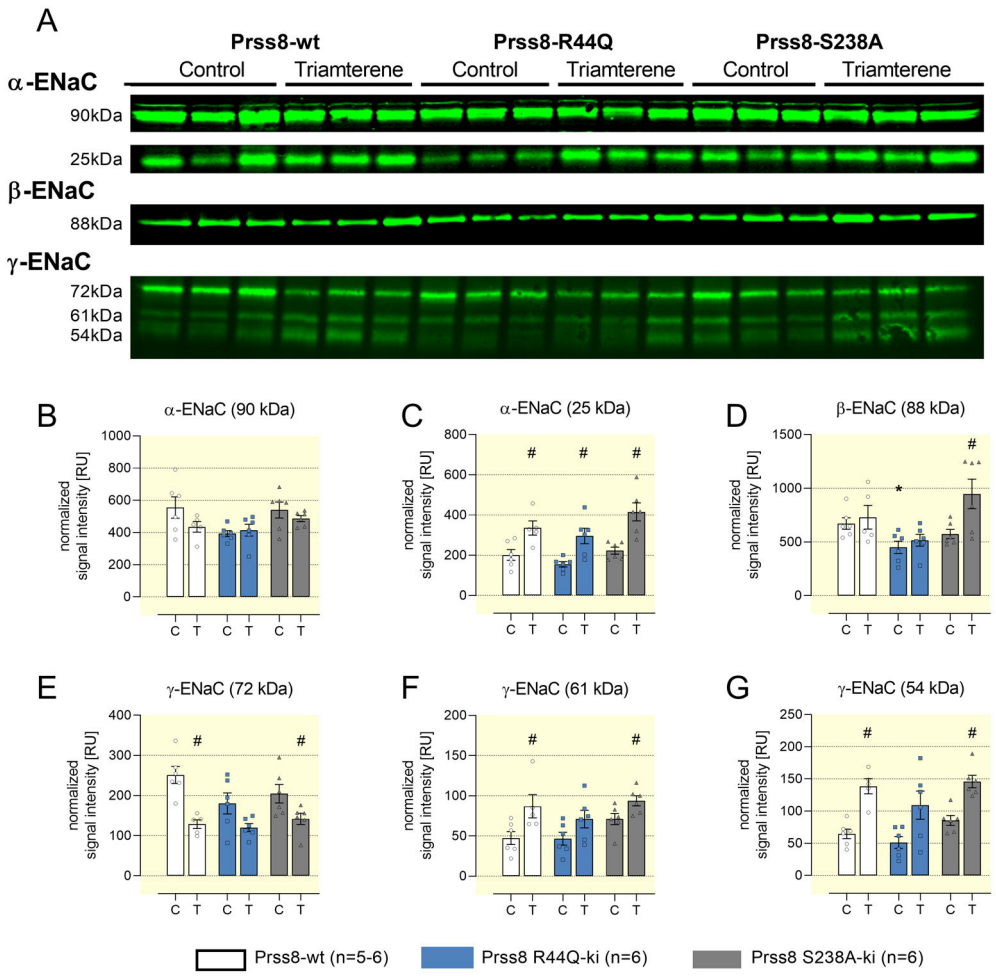

Figure 7. Protein expression of ENaC subunits in kidneys from Prss8-wt, Prss8-S238A and Prss8-R44Q mutant mice under control and triamterene treatment

A Representative Western blot for α-, β-ENaC from native kidney lysates and γ-ENaC from deglycosylated kidney lysates. Full length α-, β-, and γ-ENaC migrate at 90, 88 and 72 kDa, respectively. Furin-cleaved α- and γ-ENaC migrate at 25 and 61 kDa, respectively. Fully cleaved γ-ENaC migrates at 54 kDa.

B-G Densitometric analysis of the obtained bands after normalization for total protein content of each lane. N=5-6 for each genotype and treatment obtained from 2 gels of which one is shown.

# indicates significant difference between control and triamterene treatment, * indicates significant difference between the genotypes

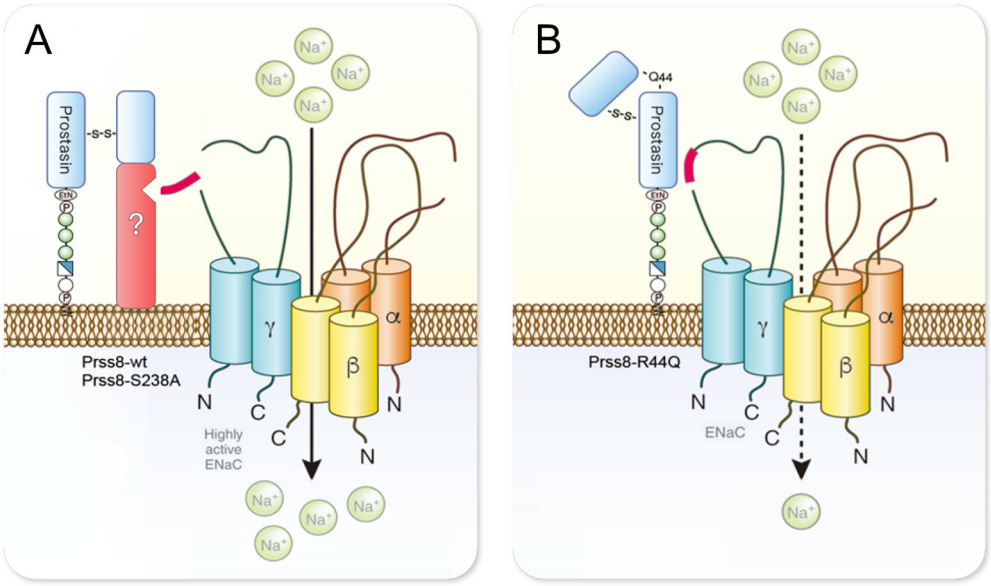

Figure 8: Model of the proteolytic ENaC activation by prostasin in the kidney

A Cleavage of Prss8 at R44 during intracellular maturation induces a conformational change to a two-chain form that enables the recruitment of another serine protease (depicted in red) to the cell surface and facilitates proteolytic activation of ENaC. This scaffold function of prostasin is independent of its proteolytic activity of prostasin as the effect of proteolytically inactive Prss8-S238A on ENaC is similar to that of Prss8-wt. The exact identity of the recruited serine protease is unknown.

B The scaffold function is impaired in zymogen-locked prostasin (Prss8-R44Q) and there is no recruitment of another serine protease. This is most likely to due to a different conformation of single-chain prostasin with the intact activation bond.

Table 1:

Plasma values of Prss8-wt, Prss8-R44Q and Prss8-S238A mutant mice before and after triamterene treatment

	control			+ triamterene		
	Prss8-wt	**Prss8 R44Q**	**Prss8 S238A**	**Prss8-wt**	**Prss8-R44Q**	**Prss8-S238A**
N	9-13	5-7	6	21-24	12-16	12-14
Na^+ [mmol L^{-1}]	150 ± 1	150 ± 1	149 ± 0.4	149 ± 1	156 ± 3 *	148 ± 2
K^+ [mmol L^{-1}]	4.3 ± 0.1	3.8 ± 0.1 *	4.4 ± 0.1	5.5± 0.3 $^{\#}$	6.6 ± 0.5 $^{\#}$	5.6 ± 0.4 $^{\#}$
pH	7.29 ± 0.01	7.21 ± 0.02 *	7.29 ± 0.01	7.17 ± 0.02 $^{\#}$	7.01 ± 0.03 $^{\#*}$	7.20 ± 0.03
pCO_2 [mmHg]	45 ± 2	56 ± 3 *	46 ± 2	52 ± 2 $^{\#}$	66 ± 3 *	52 ± 1 $^{\#}$
std HCO_3^- [mmol L^{-1}]	20 ±0.5	21 ± 1	21 ± 0.5	16 ± 1 $^{\#}$	12 ± 1 $^{\#*}$	18 ± 1
hematocrit [%]	46 ± 1	45 ± 1	47 ± 1	56 ± 1 $^{\#}$	57 ± 1 $^{\#*}$	52 ± 1 $^{*\#}$
urea [mg dL^{-1}]	44 ± 6	52 ± 9	40 ± 10	96 ± 14 $^{\#}$	199 ± 26 $^{\#*}$	111 ± 18 $^{\#}$
aldosterone [pg mL^{-1}]	225 ± 39	339 ± 118	185 ± 42	1673 ± 263 $^{\#}$	3767 ± 852 $^{\#*}$	1597 ± 344 $^{\#}$

Arithmetic means ± SEM from venous blood gas analysis (under isoflurane narcosis) and direct determination (urea, aldosterone) before and at the end of the 4 day treatment with triamterene. In some of the Prss8-R44Q mice, blood was collected before premature termination of the experiments after the 2nd or 3rd day of triamterene treatment. Std $HCO3^-$ denotes $HCO3^-$ normalized for a pCO_2 of 40 mm Hg.

$^{\#}$indicates significant difference between control and triamterene treatment

*indicates significant difference between the genotypes